Journal of Experimental Botany, Vol. 64, No. 7, pp. 1817–1827, 2013
doi:10.1093/jxb/ert069 Advance Access publication 5 April, 2013

Journal of Experimental Botany
www.jxb.oxfordjournals.org

RESEARCH PAPER

Response of green reflectance continuum removal index to the xanthophyll de-epoxidation cycle in Norway spruce needles

Daniel Kováč,[1,*], Zbyněk Malenovský[2,3], Otmar Urban[1], Vladimír Špunda[1,4], Jiří Kalina[4], Alexander Ač[1], Věroslav Kaplan[1] and Jan Hanuš[1]

[1] Global Change Research Centre, Academy of Sciences of the Czech Republic, Bělidla 4a, CZ-603 00 Brno, Czech Republic
[2] School of Geography and Environmental Studies, University of Tasmania, Private Bag 76, Hobart 7001, Australia
[3] Remote Sensing Laboratories, Department of Geography, University of Zürich, Winterthurerstrasse 190, CH-8057 Zürich, Switzerland
[4] Department of Physics, Faculty of Science, University of Ostrava, Chittussiho 10, CZ-71000 Slezská Ostrava, Czech Republic

*To whom correspondence should be addressed. E-mail: kovac.d@czechglobe.cz

Received 6 June 2012; Revised 20 November 2012; Accepted 30 January 2013

Abstract

A dedicated field experiment was conducted to investigate the response of a green reflectance continuum removal-based optical index, called area under the curve normalized to maximal band depth between 511 nm and 557 nm ($ANMB_{511–557}$), to light-induced transformations in xanthophyll cycle pigments of Norway spruce [*Picea abies* (L.) Karst] needles. The performance of $ANMB_{511–557}$ was compared with the photochemical reflectance index (PRI) computed from the same leaf reflectance measurements. Needles of four crown whorls (fifth, eighth, 10th, and 15th counted from the top) were sampled from a 27-year-old spruce tree throughout a cloudy and a sunny day. Needle optical properties were measured together with the composition of the photosynthetic pigments to investigate their influence on both optical indices. Analyses of pigments showed that the needles of the examined whorls varied significantly in chlorophyll content and also in related pigment characteristics, such as the chlorophyll/carotenoid ratio. The investigation of the $ANMB_{511–557}$ diurnal behaviour revealed that the index is able to follow the dynamic changes in the xanthophyll cycle independently of the actual content of foliar pigments. Nevertheless, $ANMB_{511–557}$ lost the ability to predict the xanthophyll cycle behaviour during noon on the sunny day, when the needles were exposed to irradiance exceeding 1000 µmol m^{-2} s^{-1}. Despite this, $ANMB_{511–557}$ rendered a better performance for tracking xanthophyll cycle reactions than PRI. Although declining PRI values generally responded to excessive solar irradiance, they were not able to predict the actual de-epoxidation state in the needles examined.

Key words: Chlorophyll to carotenoid ratio, continuum removal, excessive irradiance, leaf reflectance, spectral index, xanthophyll cycle pigments.

Introduction

Thermal energy dissipation through the xanthophyll cycle is a photoprotective mechanism that was developed by plants to keep the delicate balance between efficient light harvesting under limited irradiance and regulated energy dissipation under excess irradiance (Adir *et al.*, 2003). The xanthophyll cycle involves the enzymatic de-epoxidation of violaxanthin (V) to zeaxanthin (Z) via antheraxanthin (A) and re-epoxidation of Z to V via A (Yamamoto, 1979; Demmig-Adams and Adams, 2006). Under high irradiation, a high proton gradient across the thylakoid membrane promotes the conversion of V into Z, whereas under low light intensities or darkness the low thylakoid proton gradient induces the epoxidation of Z into V. The photoprotective V–Z conversion lowers the energy level of the lowest excited singlet state below

© The Author [2013]. Published by Oxford University Press [on behalf of the Society for Experimental Biology]. All rights reserved.
For permissions, please email: journals.permissions@oup.com

that of chlorophyll *a* (Chl *a*), providing a sink for the excess excitation energy (Frank *et al*., 1994). Upon Z–Chl *a* enclosure, excess light energy is being released in the process called non-photochemical quenching (NPQ) of Chl *a* fluorescence in photosystem II (PSII) (Krause and Weis, 1991). Z–Chl *a* enclosure is mediated through conformational changes in PSII and the co-adjacent light-harvesting antennae complex (LHCII), which is also induced by thylakoid acidification.

The engagement of the xanthophyll cycle in regulation of photosynthesis through excess light energy dissipation in PSII has been widely documented, for instance by Pfündel and Bilger (1994). Based on this finding, the photochemical reflectance index (PRI) was proposed as a physiologically based optical index responding to changes in the xanthophyll cycle through fluctuations in 531 nm reflectance (Gamon *et al*., 1992). Measurements of individual leaves have demonstrated a significant PRI relationship to the effective PSII quantum yield (Φ_{PSII}), a fluorescence-based indicator of PSII light use efficiency (LUE), and also to LUE calculated from gas exchange measurements in leaves of several species (Peñuelas *et al*., 1995). A strong PRI reduction was observed simultaneously with severe LUE reduction during midday in long-living and slow-growing evergreens having a higher maximal capacity for flexible thermal dissipation due to the possession of a higher VAZ pigment pool size (Peñuelas *et al*., 1995; Peguero-Pina *et al*., 2008). On the other hand, several studies applying PRI at canopy level showed that the relationship between photosynthetic efficiency and PRI is inconsistent over time, probably due to the changes in foliar pigment content and canopy architecture (Barton and North, 2001; Filella *et al*., 2004). It has been shown that the degradation of foliar chlorophylls generally reduces PRI as a result of the relative reflectance increase at 570 nm (Moran *et al*., 2000; Sims and Gamon, 2002; Nakaji *et al*., 2006). This PRI dependency on foliage chlorophyll content and on the chlorophyll/carotenoid ratio (Chl *a*+*b*/Car *x*+*c*) was eventually used to track seasonal alterations in photosynthetic activity (Stylinski *et al*., 2002; Filella *et al*., 2009).

A potential use of continuum-removed reflectance of green wavelengths for tracking the xanthophyll cycle dynamics was tested in previous laboratory experiments with Norway spruce seedlings (Kováč *et al*., 2012). The spectral index named area under the curve normalized to maximal band depth (ANMB) (Malenovský *et al*., 2006*b*) was calculated from leaf reflectance spectra between 510 nm and 555 nm (borders of the wavelength interval ±3 nm). ANMB was found to follow alterations in the leaf xanthophyll de-epoxidation state (DEPS), while staying insensitive to the actual content of foliar pigments (i.e. total chlorophylls, Chl *a*+*b*/Car *x*+*c* ratio, and VAZ pool size). These results were obtained from the analysis of >200 spruce needle reflectance measurements recorded after the acclimation of spruce seedlings to controlled pre-defined microclimatic conditions inside laboratory growth chambers.

The main objective of this study is, therefore, to explore the behaviour of the ANMB index in the case of mature Norway spruce [*Picea abies* (L.) Karst.] trees that are exposed to complex outdoor environmental conditions and forced to adapt quickly to different diurnal irradiation regimes. The field experiment focuses on investigating the relationship between the xanthophyll cycle dynamics and both ANMB and PRI under uncontrolled varying natural illumination conditions of a cloudy and a sunny day.

Materials and methods

Plant material and experimental design

The experiment was conducted in the forest stand located at the Experimental ecological site Bílý Kříž (Beskydy Mountains, 49°33'N, 18°32'E, northeast of the Czech Republic, 908 m a.s.l.). The experimental forest stand of 6.2 ha was planted in 1981 with 4-year-old seedlings of *P. abies* (L.) Karst. on a slope ranging from 11 ° to 16 ° with south southwest exposure. The stand density was, at the time of the experiment, ~1430 trees ha^{-1}, with the hemi-surface leaf area index (LAI) equal to 9.5 m^2 m^{-2} with a standard deviation (SD) of ±0.27 m^2 m^{-2}. The mean tree height was 13.4 m (SD ±0.1 m).

The measurements were performed on two days in July 2008 with different sky conditions: a prevailingly cloudy and a sunny day (Fig. 1). During the first measurement day, the diffuse to total irradiation ratio (DI; diffuse index) was mostly >0.7, whereas during the sunny periods of the second day it was <0.3 (Fig. 1B). The average microclimatic conditions during the 3 d preceding the measurements were similar to those on the measurement day (data not shown). Additionally, rather heavy rain was falling for those 3 d prior to the measurements on the cloudy day (total 3 d precipitation of 73 mm), whereas it was not raining for 4 d prior to the measurements on the sunny day.

Needles of different types and age classes with south southwest orientation were selected for the measurements: from the fifth whorl (counted from the apex top of the tree), 1-year-old shoots; from the eighth and 10th whorl, 2-year-old shoots; and from the 15th whorl, shoots older than 2 years. The measurement of the needle samples was performed four times throughout the day, namely approximately at dawn (D; ~05:00 h GMT+1), morning (M; ~08:00 h GMT+1), noon (N; ~13:00 h GMT+1), and afternoon (A; ~18:00 h GMT+1). Parts of the needle samples removed from the tree were measured for their optical properties and the other parts were stored in liquid nitrogen for the laboratory pigment analysis. In an effort to capture the investigated daily dynamics as accurately as possible, the needle optical properties were measured immediately after removing the shoots from the tree. Arranging the needles in the carrier for the optical property measurements took ~5 min. All measurements were completed within 10 min after removing the needles from the shoot. Previous laboratory tests showed no significant change in DEPS of spruce needles within 10 min after their detachment from the shoot (unpublished data). Therefore, the processing time is considered to be short enough to prevent any significant change in the leaf xanthophyll composition. Needles collected for the pigment analysis were weighed and their projected area was acquired using a digital table scanner. To readapt to the irradiation conditions before their collection, for the following 10 min they were exposed to irradiation of the same intensity as recorded during the *in situ* measurement with a LI-190 (Li-Cor, Lincoln, NE, USA) quantum sensor (Fig. 1C, D). Light-adapted needles were stored frozen in liquid nitrogen until they were processed for pigment analysis in the laboratory.

Reflectance measurements

Since coniferous leaves are small and narrow objects, Daughtry's method described in Mesarch *et al*. (1999) and adjusted for narrow and short Norway spruce needles by Malenovský *et al*. (2006*a*) was applied to measure the leaf optical properties. The determination of spruce needle reflectance was based on the comparison of the total sample reflectance flux (R_{TOTAL}) against the reflectance of a $BaSO_4$ reference panel (R_{REF}), both measured separately inside an

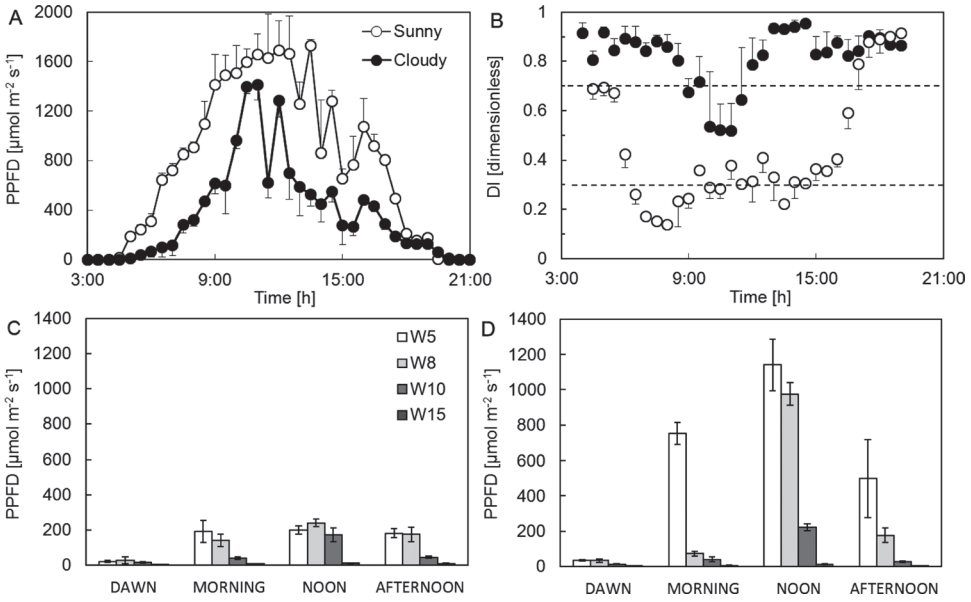

Fig. 1. Diurnal course of (A) photosynthetic photon flux density (PPFD) during the investigated cloudy and sunny days as recorded by the quantum sensor LI-190SA placed above the canopy, and (B) diffuse index (DI). The means (dots) and standard deviations (error bars) of 30 min intervals are presented. Light environment at the level of the fifth (W5), eighth (W8), 10th (W10) and 15th (W15) whorls during the time of measurement on the (C) cloudy day and (D) sunny day as recorded by the LI-190SA sensor. Presented as mean and standard deviations of three measurements performed.

integrating sphere LI-1800–12 (Li-Cor) coupled with a field spectroradiometer ASD FieldSpec-3 (ASD Inc., Colorado, USA). The spruce needle directional-hemispherical reflectance (R) between 400 nm and 1100 nm, with a wavelength interval of 1 nm, was calculated according to the equation:

$$R = \frac{R_{TOTAL}/R_{REF}}{1-GF} \quad (1)$$

where GF is the gap fraction; that is, the fraction of the air gaps between the needles of the sample measured in reflectance mode. To obtain the GF of illuminated needles, the sample holder with needles inside was placed in a conventional double lamp table scanner and an image of area illuminated during the reflectance measurement was acquired. The determination of the GF was done by dividing the number of pixels of all the gaps between the needles by the number of pixels of the illuminated area in an image processing software. The scanned needles were not used for any further analysis. The GF values of the measured samples ranged from 0.2 to 0.3. Finally, the PRI was calculated from the leaf reflectance (R_λ) of two wavelengths (λ ~531 nm and 570 nm) as $PRI = (R_{531}-R_{570})/(R_{531}+R_{570})$.

Optical index ANMB$_{511–557}$

The ANMB depth between 511 nm and 557 nm ($ANMB_{511–557}$) is an optical index based on the mathematical transformation of reflectance features called continuum removal (Kokaly and Clark, 1999; Broge and Leblanc, 2001). The detailed description of ANMB index design can be found in Malenovský *et al.* (2006*b*) and recently also in Kováč *et al.* (2012). The $ANMB_{511–557}$ calculation consists of two consecutive steps. In the first, the area under curve of continuum-removed reflectance between 511 nm and 557 nm ($AUC_{511–557}$) is calculated according to the equation:

$$AUC_{511–557} = \frac{1}{2}\sum_{i=1}^{n-1}(\lambda_{i+1}-\lambda_i)(R_{CR(\lambda i+1)}+R_{CR(\lambda i)}) \quad (2)$$

where $R_{CR(\lambda i)}$ and $R_{CR(\lambda i+1)}$ are the continuum-removed reflectance values of the spectral bands at the wavelengths λ_i and λ_{i+1} located within the spectral interval 511–557 nm (spectral resolution of 1 nm), and n is the number of spectral bands, which is, in this case, equal to 47.

In the second step, the $ANMB_{511–557}$ index is computed as the ratio of $AUC_{511–557}$ and a maximal band depth of the continuum-removed reflectance between 511 nm and 557 nm ($MBD_{511–557}$):

$$ANMB_{511–557} = \frac{AUC_{511–557}}{MBD_{511–557}} \quad (3)$$

The reflectance of the selected wavebands is influenced by conversion of the xanthophyll cycle pigments, which was first detected and reported as leaf reflectance fluctuation at 526 nm by Gamon *et al.* (1997). Making use of several bands of the green spectral region combined within the $ANMB_{511–557}$ index was found to be yet another efficient way to retrieve information on the rate of xanthophyll de-epoxidation (Kováč *et al.*, 2012).

Foliar pigment analysis

The light-adapted needle samples, transported frozen in liquid nitrogen to the laboratory, were homogenized in 80% acetone with a small amount of $MgCO_3$, and centrifuged (480 rpm) at room temperature for 3 min. The contents of Chl *a*, Chl *b*, and total carotenoids (Car *x*+*c*) in the supernatant were determined spectrophotometrically (UV/VIS 550, Unicam, Cambridge, UK) from absorbances measured at 470, 646.8, 663.2, and 750 nm according to the equations presented by Lichtenthaler (1987). Chl *a*+*b* and Car *x*+*c* contents were expressed per unit needle area that was estimated via scanned digital images of samples analysed by the Cernota software (Kalina and Slovák, 2004). The relative amounts of the xanthophyll cycle pigments, antheraxanthin (A), violaxanthin (V), and zeaxanthin (Z), were obtained from HPLC pigment analyses (Kurasová *et al.*, 2003). The conversion factors for contents of the individual carotenoids (i.e. the pool of the xanthophyll cycle pigments; VAZ) and

chlorophylls were applied according to Färber and Jahns (1998). The conversion state of the xanthophyll cycle pigments (i.e. de-epoxidation state; DEPS) was calculated according to Gilmore and Björkman (1994) as:

$$DEPS=[A+Z]/[V+A+Z] \quad (4)$$

Statistical data analysis

Statistically significant differences of means were tested using a two-sample *F*-test for variances, followed by a Student's *t*-test with the level of significance $P < 0.05$. Based on the results of the *F*-test, a *t*-test, assuming either equal or unequal variances, was applied.

The determination coefficient (R^2) was computed to express the percentage variation of a dependent variable explained by an established regression to the independent variable. The significance of the statistical model was tested at probability levels $P < 0.05$, $P < 0.01$, and $P < 0.001$, using analysis of variance (ANOVA).

All calculations and tests were conducted in the R mathematical–statistical programming environment (R Development Core Team, 2010).

Results and Discussion

Composition of photosynthetic pigments in needle samples during the sunny and cloudy day

Plant material collected from each level of the spruce crown differed in the morphometric parameter specific leaf area (SLA). On both experimental days, the highest SLA values were observed for needles of the 10th whorl, and the lowest for needles of the fifth and the eighth whorls (Fig. 2A; $P < 0.05$).

The total chlorophyll content (Chl *a*+*b*) in needles collected from each crown level during the sunny and cloudy day varied within the range shown in Fig. 2B. Chl *a*+*b* of the fifth and eighth whorl sampled on the sunny day was on average ~0.05 g m^{-2} higher than Chl *a*+*b* examined on the cloudy day ($P < 0.05$). This difference increased the Chl *a*+*b*/Car *x*+*c* ratio in needles of the fifth whorl on the sunny day (Fig. 2D; $P < 0.05$), whereas the Chl *a*+*b*/Car *x*+*c* ratio in needles of the eighth whorl remained within the original range of the cloudy day. Similarly, needles from mostly shaded lower levels of the crown (10th and 15th whorl) did not exhibit significant Chl *a*+*b*/Car *x*+*c* differences between both experimental days (Fig. 2D). Their Chl *a*+*b*/Car *x*+*c* ratios are consistent with the previous finding of Sarijeva *et al.* (2007) suggesting that the Chl *a*+*b*/Car *x*+*c* ratio of shaded leaves is higher due to possession of a greater amount of LHCII.

The pool size of the xanthophyll cycle pigments (VAZ) clearly follows the sun to shade crown gradient, being larger in sunlit and smaller in shaded leaves (Fig. 2C; $P < 0.05$). The statistically significant difference highlights the importance of the xanthophyll cycle for photoprotection in each particular needle type (Demmig-Adams, 1998). In sunlit needles, VAZ/Chl *a*+*b* is similar for needles sampled on the sunny day despite the increase in Chl *a*+*b*. Although not statistically different, the VAZ pool in needles of the fifth whorl increased slightly on the sunny day compared with the pool on the cloudy day.

Dynamic conversions of the xanthophyll cycle pigments during the cloudy and sunny day

At dawn (D) of both days, the needle DEPS of all whorls was nearly the same, namely ~15% (Fig. 3). As expected and observed previously (Demmig-Adams *et al.*, 1999), zeaxanthin reached the maximal conversional state during noon under both sky conditions. The highest conversional rate of xanthophyll cycle pigments was found on the sunny day in sunlit needles of the fifth and eighth whorl (Fig. 3B). In this

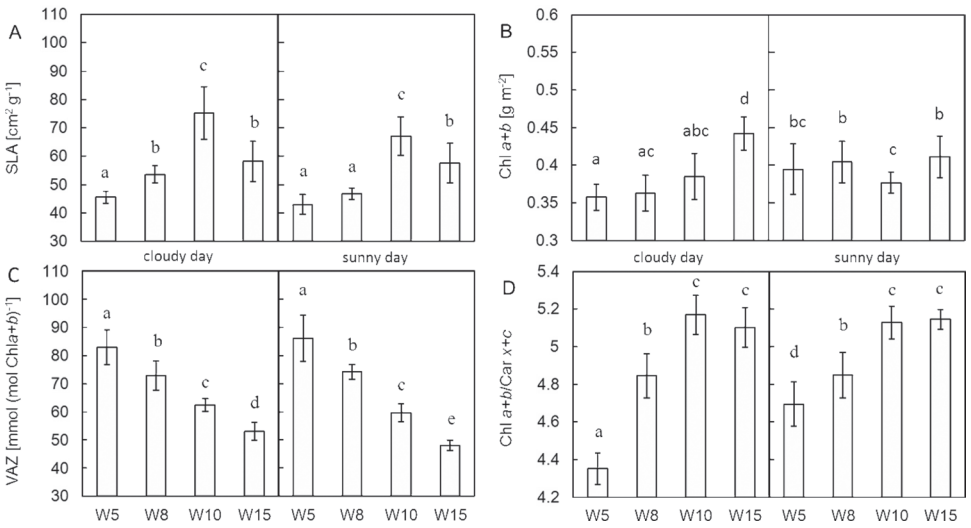

Fig. 2. Difference in (A) specific leaf area (SLA), (B) amount of chlorophyll *a*+*b* per unit leaf area, (C) content of xanthophyll cycle pigments (VAZ) per total amount of chlorophylls, and (D) ratio of total chlorophylls to total carotenoids (Chl *a*+*b*/Car *x*+*c*) in needles within each examined level (whorls W5, W8, W10, and W15) of spruce crowns. Values presented show the means ±SD (vertical bars) of data measured during the cloudy day (left column) and the sunny day (right column). Data followed by the same letter indicate a non-significant statistical difference ($P > 0.05$; Student's *t*-test) (n=20).

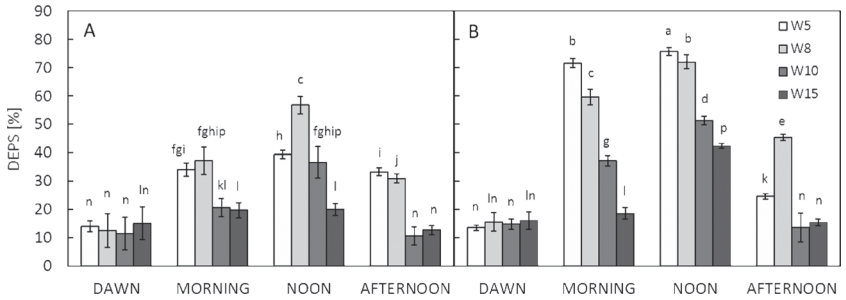

Fig. 3. Diurnal changes in the de-epoxidation state of xanthophyll cycle pigments (DEPS) in needles from the fifth, eighth, 10th, and 15th whorl (W) on (A) the cloudy day and (B) the sunny day. Means (columns) and standard deviations (vertical bars) are presented (n=5). Data followed by the same letter indicate statistically non-significant differences ($P > 0.05$; Student's t-test).

part of the crown, DEPS in the morning (M) of the sunny day reached values of ~60–70%. DEPS between 70% and 75% was peaking at noon (N) under the irradiance of ~1000 µmol m^{-2} s^{-1}. In the late afternoon (A), the DEPS dropped down to 25% and 45% in needles of the fifth and eighth whorl, respectively.

A relatively low noon DEPS of 39.3% in needles of the fifth whorl after a relatively clear sky window between 09:30 h and 11:30 h on the cloudy day (Fig. 1A) is comparable with a morning DEPS of 34.1% (Fig. 3A). The DEPS did not increase significantly or quickly relaxed close to the morning state. Either way, it did not persist at a high level as usually observed after a high solar illumination in conditions of an additional stress, such as intensive drought (Baraldi *et al.*, 2008). This suggests that during the present experiment the examined tree was not stressed by any other environmental factor except high irradiance. At noon on the cloudy day, the DEPS of 56% in needles of the eighth whorl (Fig. 3A) was accompanied by possession of a low pool of VAZ pigments. In this particular case, the Chl $a+b$ of eighth whorl needles was 2% lower compared with that in fifth whorl needles, and the VAZ/Chl $a+b$ ratio of fifth whorl needles was 12% higher ($P < 0.05$) than that in needles of the eighth whorl. Finally, for both days, the DEPS diurnal patterns of 10th and 15th whorl needles were similar to that observed in sunlit needles of the fifth and eight whorls, but with a lower VAZ conversional state (Fig. 3).

Photochemical reflectance index (PRI)

Mean reflectance spectra collected for needles of all four whorls investigated during both experimental days are shown in Fig. 4. Standard error bars indicate the reflectance variability at wavelengths of 550 nm and 800 nm. The shape and amplitude of the needle reflectance signatures indicate systematic changes in foliar pigments and also in geometrical and structural needle characteristics as previously observed by Malenovský *et al.* (2006*a*). Even though pigment analyses were not performed on plant material used for optical measurements, the causal correspondence that can be observed between the visible and near infrared reflectance in Fig. 4 and pigment content and SLA measurements in Fig. 2 displays a good representation of spectral signatures for each crown level.

Diurnal courses of the PRI index computed from needle directional-hemispherical reflectance of the four investigated whorls acquired during the cloudy and sunny day are shown in Fig. 5. PRI values are positive in most cases, which is in accordance with the results reviewed in Garbulsky *et al.* (2011). Negative PRI values were typically reported for leaves under strong light stress, which induces photoprotective reactions resulting in low LUE. In the present experiment these would be needles of the fifth and eighth whorl in late morning, noon, and afternoon on the sunny day. PRI was, however,

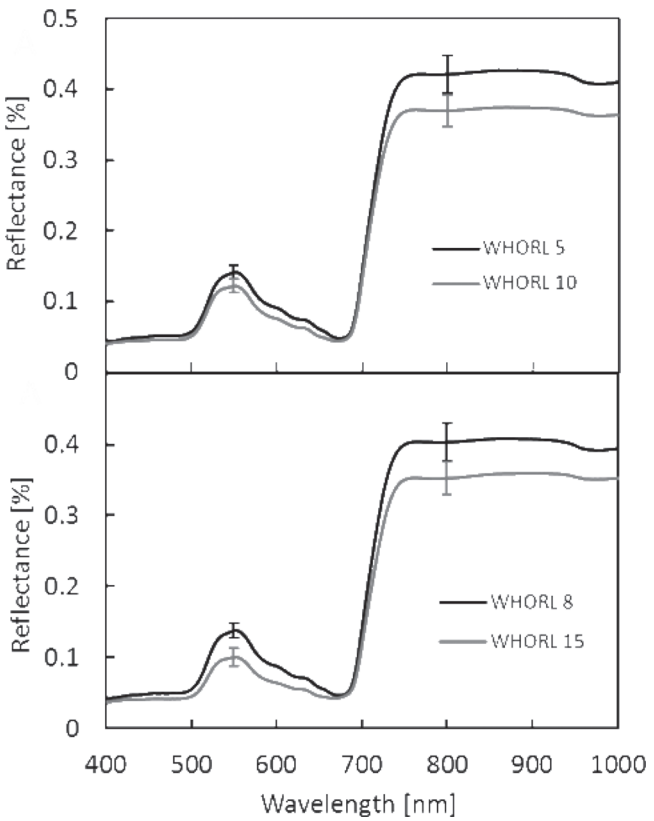

Fig. 4. Reflectance spectra of spruce needle samples measured during both experimental days within each crown level. The curve indicates the mean of 24 needle measurements performed for each whorl during both days; error bars indicate two-sided standard deviations in reflectance at 550 nm and 800 nm.

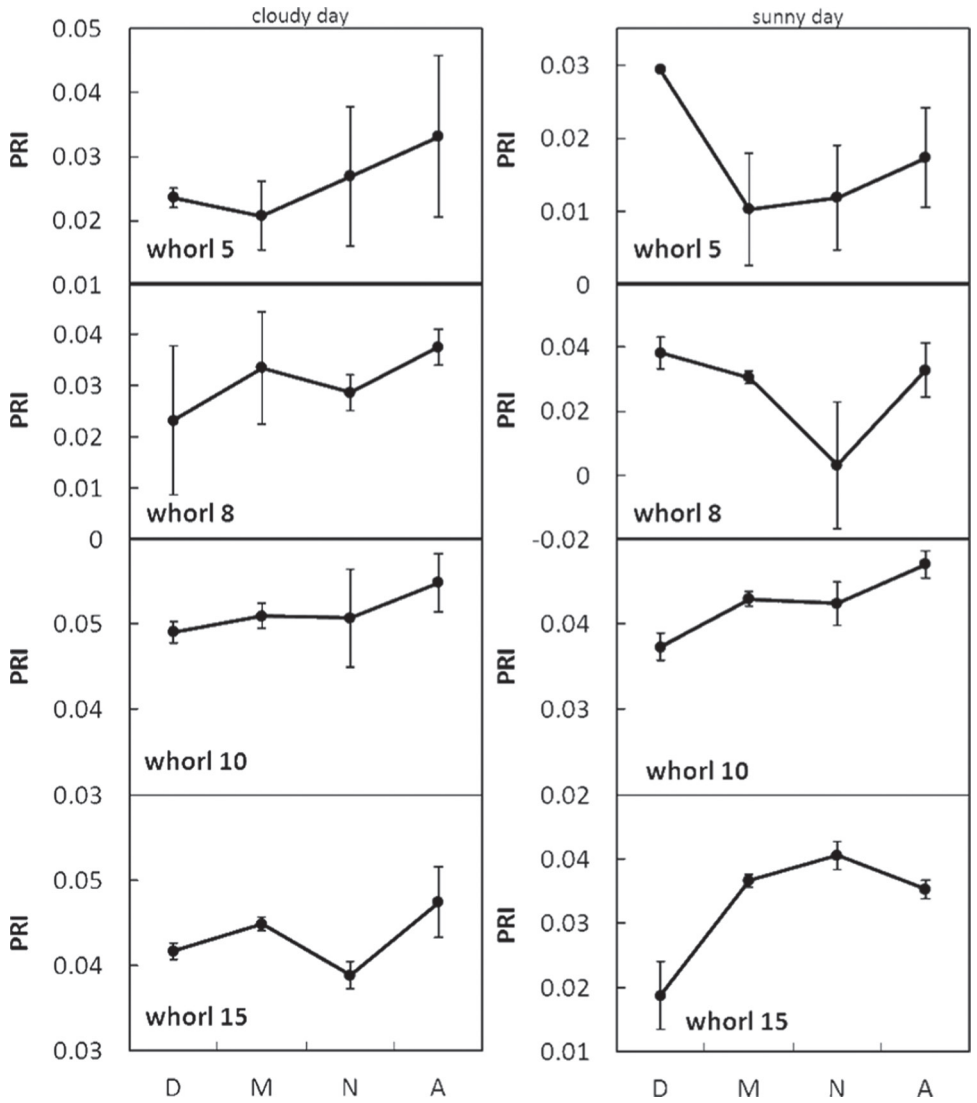

Fig. 5. Diurnal course of the PRI index calculated from needle reflectance measurements on needles from the fifth, eighth, 10th, and 15th whorl during the cloudy and sunny day. Each dot represents the mean of three measurements performed per whorl and time, and vertical bars show ±SD. D, dawn; M, morning; N, noon; and A, afternoon.

reaching negative values only for needles of the eighth whorl at noon; for the remaining needle samples it was close to zero, but positive. Also, expected daily changes in PRI due to the increasing solar irradiation are not obvious (Fig. 5). This can be explained by the fact that PRI values are not functionally dependent only on xanthophyll de-epoxidation, but also on the actual pool of carotenoids and chlorophylls (Sims and Gamon, 2002). Results in Fig. 6 show that the PRI values obtained are in general lower for foliage experiencing a stronger light with the photosynthetic photon flux density (PPFD) reaching or exceeding 1000 µmol m^{-2} s^{-1} (i.e. fifth and eighth whorl on the sunny day) and having a lower Chl *a*+*b*/Car *x*+*c* ratio (Cheng *et al.*, 2012). Higher PRI values can indicate either medium DEPS combined with a lower Chl *a*+*b*/Car *x*+*c* ratio or low DEPS combined with a higher Chl *a*+*b*/Car *x*+*c* ratio (compare Figs 3 and 6). Consequently, the interpretation of the PRI values measured under a PPFD of <300 µmol m^{-2} s^{-1} (i.e. all whorls on the cloudy day and the 10th and 15th whorl on the sunny day; Fig. 1) is ambiguous due to the differences in pigment content. This ambiguity may also explain an insignificant regression relationship that was observed between the PRI and DEPS measurements (results not shown).

ANMB$_{511–557}$ index

ANMB$_{511–557}$ was designed as the ratio of the area under the continuum-removed reflectance between 511 nm and 557 nm (AUC$_{511–557}$) and the depth of this feature (MBD$_{511–557}$) (Equation 3). Although AUC$_{511–557}$ carries valuable information about reflectance losses caused by xanthophyll de-epoxidation, it is also influenced by the fluctuation of green reflectance due to the varying chlorophyll pigment composition and mass (Fig. 4). Consequently AUC$_{511–557}$ and also MBD$_{511–557}$ do not exhibit a strong dependence on DEPS (Fig. 7), but being shaped by similar driving forces their ratio

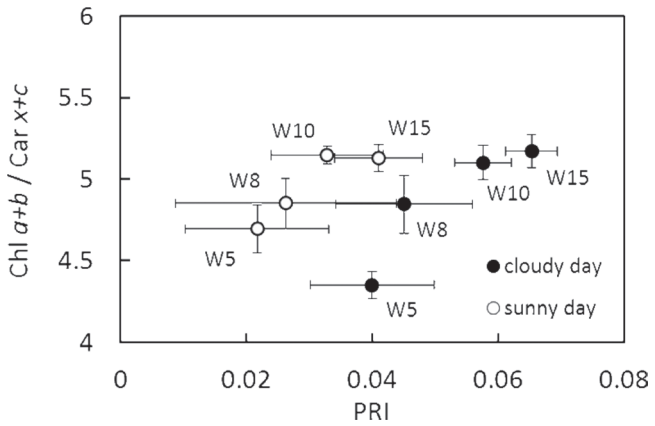

Fig. 6. Relationship between PRI values retrieved from 12 reflectance measurements of the four investigated crown whorls (fifth, eighth, 10th, and 15th whorl from the crown top) and Chl *a+b*/Car *x+c* ratios of these needles as averaged from 20 measurements conducted on the cloudy and sunny day. Error bars indicate the measurement standard deviation.

is able to eliminate the undesirable influence of chlorophyll and to emphasize a tiny xanthophyll de-epoxidation signal carried by $AUC_{511–557}$. Figure 8 clearly shows the systematic difference between $AUC_{511–557}$ normalized by $MBD_{511–557}$ for DEPS equal to 13.5, 34.1, and 71.6%. The main advantage of the ANMB method is in avoidance of the reflectance at 570 nm, which has been identified as the cause of PRI instability by Moran *et al.* (2000) and later by Nakaji *et al.* (2006). As illustrated in Fig. 6, the PRI values are dependent on differences in leaf Chl *a+b* and Car *x+c* pigment pools; the amount of chlorophyll determines the reflectance amplitude at 570 nm.

Diurnal changes of the $ANMB_{511–557}$ index during both experimental days are displayed in Fig. 9. Graphs shows that the $ANMB_{511–557}$ values of the fifth, eighth, and 10th whorl needles follow the alterations in xanthophyll DEPS (Fig. 3) during the cloudy day as well as do those of the 10th whorl needles sampled on the sunny day. Needles of the 15th whorl, however, do not show the diurnal pattern of $ANMB_{511–557}$ following temporal changes in DEPS, which might be caused by their low content of xanthophyll cycle pigments (VAZ) in general (see Fig. 2C). Similarly, no relationship to DEPS was found for the needles of the fifth and eight whorls on the sunny day due to the strong outlying deviation in $ANMB_{511–557}$ diurnal behaviour observed at noon.

These results confirm, in general, previous findings showing the ability of the ANMB index to assess the dynamics of the xanthophyll cycle in needles of spruce seedlings kept under controlled and systematically varied environmental conditions (Kováč *et al.*, 2012). In contrast to this laboratory study, the $ANMB_{511–557}$ field measurements deviate from the expected diurnal course in the case of sunlit needles (the fifth and eighth whorls) during noon of the sunny day. Although the PPFD of both experiments reached up to 1000 µmol m^{-2} s^{-1} (Fig. 1D), the field ANMB values suddenly increased due to the unexpected drop in $MBD_{511–557}$. At this stage, an explanantion for this mismatched ANMB behaviour cannot be found. Based on the findings of previous studies (Nichol *et al.*, 2000), it is assumed that other physiological processes regulating the plant's photosynthetic capacity, for example non-assimilatory electron transport (Munekaga *et al.*,

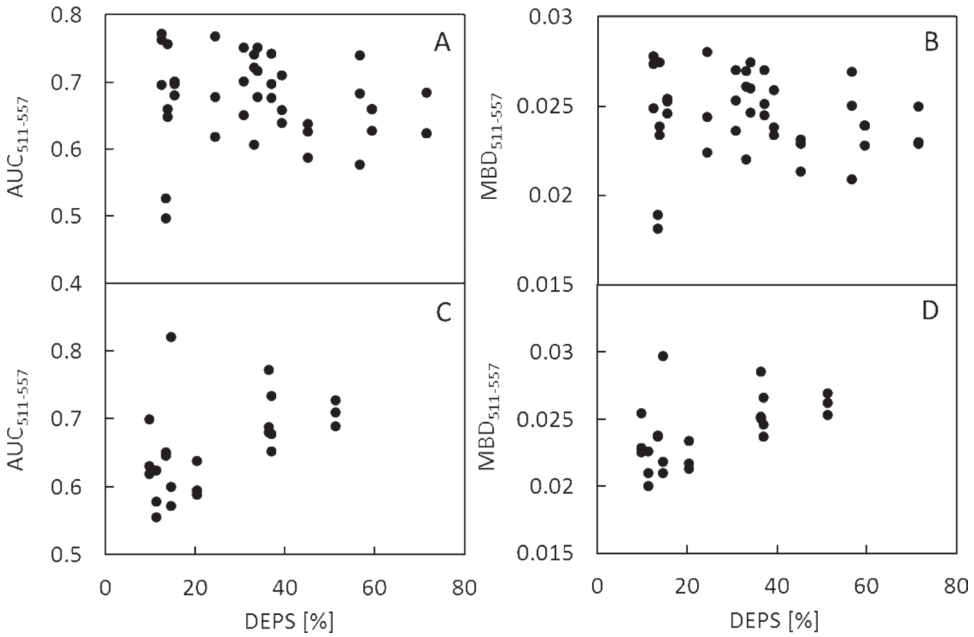

Fig. 7. Relationship between the de-epoxidation state of xanthophyll cycle pigments (DEPS) and area under the curve (AUC) and maximal band depth (MBD) of continuum-removed reflectance of the fifth and eighth whorl needles (A and B, *n*=42) and the 10th whorl needles (C and D, *n*=24) between 511 nm and 557 nm. Data for the 15th whorl are not shown due to insufficient sensitivity of the $ANMB_{511–557}$ index to DEPS.

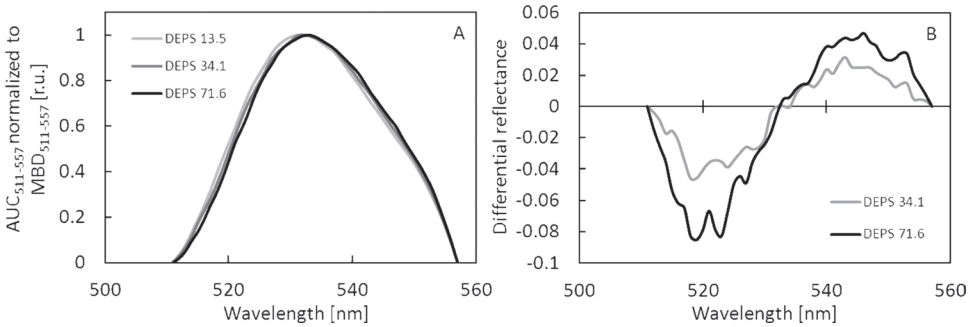

Fig. 8. (A) Area under the curve (AUC) of continuum-removed reflectance of Norway spruce needles between 511 nm and 557 nm normalized to maximal band depth (MBD) of $AUC_{511–557}$. (B) Normalized area under continuum-removed reflectance of two needle samples with de-epoxidation state of xanthophyll cycle pigments (DEPS) equal to 34.1% and 71.6%, respectively, subtracted from the needle sample with DEPS of 13.5%.

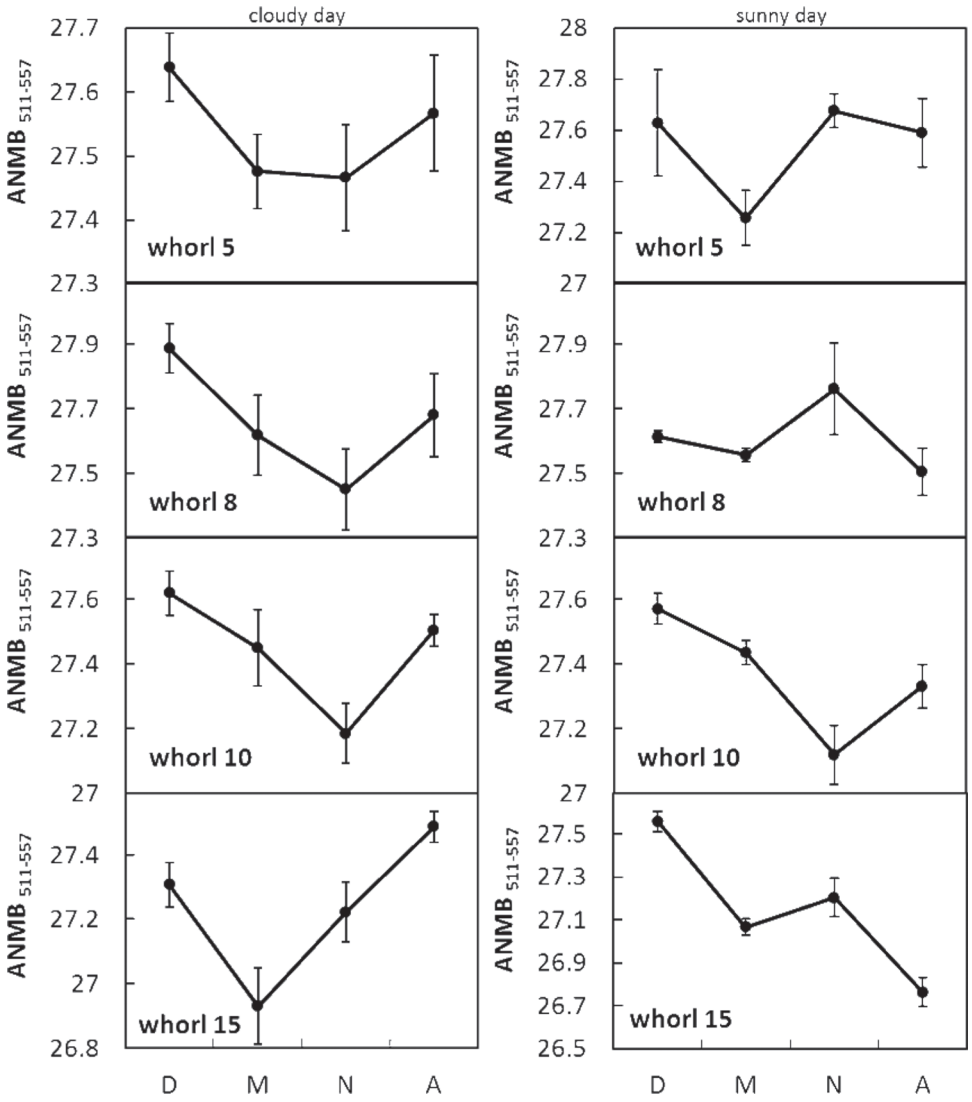

Fig. 9. Diurnal course of the $ANMB_{511–557}$ index calculated from the reflectance measured of needles from the fifth, eighth, 10th, and 15th whorl during the cloudy and the sunny day. Each dot represents the mean of three measurements performed per whorl and time. Vertical bars show ±SD. D, dawn; M, morning; N, noon; and A, afternoon.

2004) or photorespiration (Kangasjarvi *et al.*, 2012), may interfere with the indicative ability of $ANMB_{511–557}$. The fact that the cause is at this point unknown suggests that follow-up experiments focusing on plant physiological differences between both experiments are needed to investigate this phenomenon.

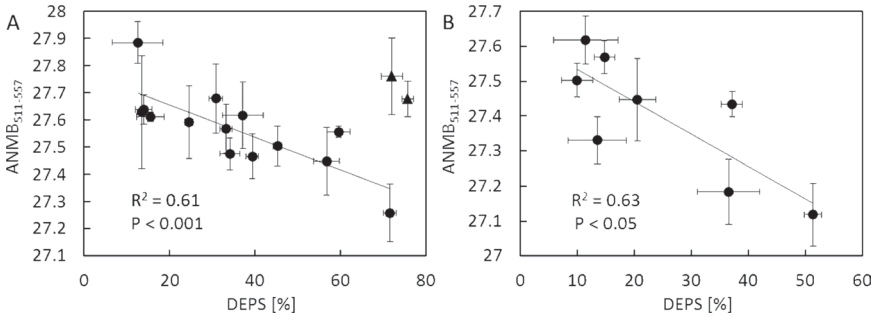

Fig. 10. Dependency between mean values of $ANMB_{511–557}$ and DEPS in (A) needles of the fifth and eighth whorl together (n=14) (noon collections displayed as triangles were excluded from R^2 computation) and (B) needles of the 10th whorl (n=8). Average values ±SD of the vegetation indices were calculated from three leaf reflectance signatures, and average DEPS values ±SD were calculated from five samples measured during the measurement cycle in the diurnal course.

Significance of the $ANMB_{511–557}$ relationship to xanthophyll changes

Despite the fact that most of the needle $ANMB_{511–557}$ and DEPS measurements do share similar diurnal patterns, a linear regression between $ANMB_{511–557}$ and DEPS of the fifth, eighth, and 10th whorl needles was found to be insignificant. Statistically significant negative regressions were found only for values of the first two whorls corresponding to DEPS between 13% and 72% (i.e. between low and moderate PPFDs; measurements acquired at noon of the sunny day were excluded), the coefficient of the determination R^2=0.61 ($P < 0.001$), and, of the 10th whorl, the coefficient of the determination equal to 0.63 ($P < 0.05$, Fig. 10). The fact that these significant dependencies were found in needles with a considerable variability in Chl a+b and Chl a+b/Car x+c (Fig. 2) suggests that $ANMB_{511–557}$ is independent of the apparent content of foliar pigments. On the other hand, it was noticed that an increase in $ANMB_{511–557}$ of needles from the eighth whorl on the cloudy day corresponds to the increase in sample SLA (compare Fig. 2A with Fig. 9). An explanation for this correlation can be found in reflectance measurements, which were corrected for the air gap fraction between measured needles. This correction is less accurate in the case of small sized and strongly arched spruce needles (i.e. low SLA). Therefore, statistically higher SLA for the needles from the 10th whorl compared with the needles of the fifth and eighth whorls might be the reason why the $ANMB_{511–557}$ values originating from different crown levels are not comparable, even though they correspond to a similar DEPS. The influence of SLA on leaf $ANMB_{511–557}$ of broadleaf plants and coniferous species with long bifacial needles (e.g. pines) is expected to be negligible. Finally, it is acknowledged that the extension of the sampling scheme used here, that would ensure full representation of the canopy heterogeneity, might help to clarify the inconsistencies found between the optical indices and DEPS.

Perspective of the introduced $ANMB_{511–557}$ index

The experiment suggests that PRI may not be the most efficient diurnal indicator of xanthophyll cycle photoprotection. The variations of Chl a+b/Car x+c in needles measured are discussed as the possible cause of low PRI performance in tracking DEPS of each crown level examined. A number of studies also indicated that canopy PRI is dependent upon sensor viewing geometry (Hilker *et al.*, 2008; Middleton *et al.*, 2009). PRI values are higher when more shaded foliage with a higher Chl a+b/Car x+c ratio and less soil contamination is being observed (Cheng *et al.*, 2010). Taking into account only sunlit leaves leads to an underestimation of canopy PRI, relative to the actual photosynthesis performance (Goerner *et al.*, 2011). Realizing that combining information from strongly photosynthetically down-regulated sunlit foliage and less down-regulated shaded foliage is essential for correct canopy PRI interpretation, Hilker *et al.* (2010) investigated PRI dependency on sensor viewing geometry and proposed a multiangular observation algorithm estimating the LUE across different biomes. Although Malenovský *et al.* (2013) recently demonstrated the independence of a continuum removal-based optical index from the canopy leaf area index, the newly proposed $ANMB_{511–557}$ index computed for vegetation canopies observed under different sensor viewing angles will need a similar treatment. Nevertheless, as it is not sensitive to the changes in the composition of Chl a+b and Car x+c pigments, the $ANMB_{511–557}$ index is expected to provide more accurate estimation of the actual stress response to solar irradiation at the canopy scale. The first step in this direction should be improvement of the index performance for irradiances with PPFD >1000 µmol m^{-2} s^{-1}. The second step should take $ANMB_{511–557}$ through a multicriterion sensitivity analysis investigating its applicability for canopies of different structural complexity and for airborne and spaceborne observations of different spectral, spatial, and temporal specifications.

Conclusions

In this study the performance of a new spectroscopy indicator for a rapid assessment of the xanthophyll cycle state of plant leaves was investigated in the field; that means, under natural environmental conditions. The results demonstrate the possibility to track the xanthophyll de-epoxidation reactions in Norway spruce needles using the leaf reflectance continuum removal optical index termed $ANMB_{511–557}$.

Among all examined leaf characteristics, differences in the chlorophyll content and the Chl $a+b$/Car $x+c$ ratio varied most significantly when comparing sun- and shade-adapted needles. None of them was, however, found to disturb the indicative ability of $ANMB_{511–557}$. The analysis of the $ANMB_{511–557}$ dependence on DEPS proved that the index can follow the photoprotective xanthophyll changes in plant leaves during a cloudy day. $ANMB_{511–557}$ was, however, unable to capture the decreasing DEPS trend that occurred at noon on the sunny day (i.e. under the actual irradiation above 1000 µmol m^{-2} s^{-1}). This $ANMB_{511–557}$ deviation has not been explained, but it is expected to be associated with an enhanced need for plant intensive photoprotection. The observed spectral deviation in $ANMB_{511–557}$ diurnal behaviour may affect the current concept of deriving LUE from reflectance data in general (Garbulsky *et al.*, 2011), and should therefore be further investigated. Also, the improvement of $ANMB_{511–557}$ performance and its potential use for estimating leaf or even canopy LUE remain the objective of follow-up studies.

Acknowledgements

This work is a part of the research supported by the grant projects SP/2D1/70/08 (ForChange) and LD12042 (COST). This article is a product of the CzechGlobe Centre that is being developed within the OP RDI and co-financed from EU funds and the State Budget of the Czech Republic (CZ.1.05/1.1.00/02.0073). The experimental site Bílý Kříž is within the National infrastructure for carbon observations–CzeCOS/ICOS supported by the Ministry of Education CR (LM2010007). We thank Mrs Běla Piskořová and Mr Ladislav Šigut of the Department of Physics at the University of Ostrava for analysing the content of the photosynthetic pigments, and Mrs Gabrielle Johnson for English language editing.

References

Adir N, Zer H, Shochat S, Ohad I. 2003. Photoinhibition—a historical perspective. *Photosynthesis Research* **76,** 343–370.

Baraldi R, Canaccini F, Cortes S, Magnani F, Rapparini F, Zamboni A, Raddi S. 2008. Role of xanthophyll cycle-mediated photoprotection in Arbutus unedo plants exposed to water stress during the Mediterranean summer. *Photosynthetica* **46,** 378–386.

Barton CVM, North PRJ. 2001. Remote sensing of canopy light use efficiency using the photochemical reflectance index—model and sensitivity analysis. *Remote Sensing of Environment* **78,** 264–273.

Broge NH, Leblanc E. 2001. Comparing prediction power and stability of broadband and hyperspectral vegetation indices for estimation of green leaf area index and canopy chlorophyll density. *Remote Sensing of Environment* **76,** 156–172.

Cheng YB, Middleton EM, Huemmrich KF, Zhang QY, Campbell PKE, Corp LA, Russ AL, Kustas WP. 2010. Utilizing *in situ* directional hyperspectral measurements to validate bio-indicator simulations for a corn crop canopy. *Ecological Informatics* **5,** 330–338.

Cheng YB, Middleton E, Zhang Q, Corp L, Dandois J, Kustas WP. 2012. The photochemical reflectance index from directional cornfield reflectances: observations and simulations. *Remote Sensing of Environment* **124,** 444–453.

Demmig-Adams B. 1998. Survey of thermal energy dissipation and pigment composition in sun and shade leaves. *Plant and Cell Physiology* **39,** 474–482.

Demmig-Adams B, Adams WW. 2006. Photoprotection in an ecological context: the remarkable complexity of thermal energy dissipation. *New Phytologist* **172,** 11–21.

Demmig-Adams B, Adams WW, Ebbert V, Logan BA. 1999. *Ecophysiology of the xanthophyll cycle. Photochemistry of carotenoids*, Vol. **8**. Dordrecht: Kluwer Academic Publishers, 245–269.

Färber A, Jahns P. 1998. The xanthophyll cycle of higher plants: influence of antenna size and membrane organization. *Biochimica et Biophysica Acta* **1363,** 47–58.

Filella I, Peñuelas J, Llorens L, Estiarte M. 2004. Reflectance assessment of seasonal and annual changes in biomass and CO_2 uptake of a Mediterranean shrubland submitted to experimental warming and drought. *Remote Sensing of Environment* **90,** 308–318.

Filella I, Porcar-Castell A, Munne-Bosch S, Back J, Garbulsky MF, Peñuelas J. 2009. PRI assessment of long-term changes in carotenoids/chlorophyll ratio and short-term changes in de-epoxidation state of the xanthophyll cycle. *International Journal of Remote Sensing* **30,** 4443–4455.

Frank HA, Cua A, Chynwat V, Young A, Gosztola D, Wasielewski MR. 1994. Photophysics of the carotenoids associated with the xanthophyll cycle in photosynthesis. *Photosynthesis Research* **41,** 389–395.

Gamon JA, Peñuelas J, Field CB. 1992. A narrow waveband spectral index that tracks diurnal changes in photosynthetic efficiency. *Remote Sensing of Environment* **41,** 35–44.

Gamon JA, Serrano L, Surfus JS. 1997. The photochemical reflectance index: an optical indicator of photosynthetic radiation use efficiency across species, functional types, and nutrient levels. *Oecologia* **112,** 492–501.

Garbulsky MF, Peñuelas J, Gamon J, Inoue Y, Filella I. 2011. The photochemical reflectance index (PRI) and the remote sensing of leaf, canopy and ecosystem radiation use efficiencies. A review and meta-analysis. *Remote Sensing of Environment* **115,** 281–297.

Gilmore AM, Björkman O. 1994. Adenine nucleotides and the xanthophyll cycle in leaves. II. Comparison of the effects of CO_2- and temperature-limited photosynthesis on photosystem II fluorescence quenching, the adenylate energy charge and violaxanthin de-epoxidation in cotton. *Planta* **192,** 537–544.

Goerner A, Reichstein M, Tomelleri E, Hanan N, Rambal S, Papale D, Dragoni D, Schmullius C. 2011. Remote sensing of ecosystem light use efficiency with MODIS-based PRI. *Biogeosciences* **8,** 189–202.

Hilker T, Coops NC, Hall FG, Black TA, Wulder MA, Nesic Z, Krishnan P. 2008. Separating physiologically and directionally induced changes in PRI using BRDF models. *Remote Sensing of Environment* **112,** 2777–2788.

Hilker T, Hall FG, Coops NC, *et al.* 2010. Remote sensing of photosynthetic light-use efficiency across two forested biomes: spatial scaling. *Remote Sensing of Environment* **114,** 2863–2874.

Kalina J, Slovák V. 2004. The inexpensive tool for the determination of projected leaf area. *Ekologia-Bratislava* **23,** 163–167.

Kangasjarvi S, Neukermans J, Li SC, Aro EM, Noctor G. 2012. Photosynthesis, photorespiration, and light signalling in defence responses. *Journal of Experimental Botany* **63,** 1619–1636.

Kokaly RF, Clark RN. 1999. Spectroscopic determination of leaf biochemistry using band-depth analysis of absorption features and stepwise multiple linear regression. *Remote Sensing of Environment* **67,** 267–287.

Kováč D, Navrátil M, Malenovský Z, Štroch M, Špunda V, Urban O. 2012. Reflectance continuum removal spectral index tracking the xanthophyll cycle photoprotective reactions in Norway spruce needles. *Functional Plant Biology* **39,** 987–998.

Krause GH, Weis E. 1991. Chlorophyll fluorescence and photosynthesis: the basics. *Annual Review of Plant Physiology and Plant Molecular Biology* **42,** 313–349.

Kurasová I, Kalina J, Urban O, Štroch M, Špunda V. 2003. Acclimation of two distinct plant species, spring barley and Norway spruce, to combined effect of various irradiance and CO_2 concentration during cultivation in controlled environment. *Photosynthetica* **41,** 513–523.

Lichtenthaler HK. 1987. Chlorophylls and carotenoids: pigments of photosynthetic biomembranes. *Methods in Enzymology* **148,** 350–382.

Malenovský Z, Albrechtová J, Lhotáková Z, Zurita-Milla R, Clevers J, Schaepman ME, Cudlín P. 2006a. Applicability of the PROSPECT model for Norway spruce needles. *International Journal of Remote Sensing* **27,** 5315–5340.

Malenovský Z, Homolová L, Zurita-Milla R, Lukeš P, Kaplan V, Hanuš J, Gastellu-Etchegorry J-P, Schaepman M. 2013. Retrieval of spruce leaf chlorophyll content from airborne image data using continuum removal and radiative transfer. *Remote Sensing of Environment* **131,** 85–102.

Malenovský Z, Ufer CM, Lhotáková Z, Clevers JGPW, Schaepman ME, Albrechtová J, Cudlín P. 2006b. A new hyperspectral index for chlorophyll estimation of a forest canopy: area under curve normalized to maximal band depth between 650–725 nm. *EARSeL eProceedings* **5,** 161–172.

Mesarch MA, Walter-Shea EA, Asner GP, Middleton EM, Chan SS. 1999. A revised measurement methodology for conifer needles spectral optical properties: evaluating the influence of gaps between elements. *Remote Sensing of Environment* **68,** 177–192.

Middleton EM, Cheng YB, Hilker T, Black TA, Krishnan P, Coops NC, Huemmrich KF. 2009. Linking foliage spectral responses to canopy-level ecosystem photosynthetic light-use efficiency at a Douglas-fir forest in Canada. *Canadian Journal of Remote Sensing* **35,** 166–188.

Moran JA, Mitchell AK, Goodmanson G, Stockburger KA. 2000. Differentiation among effects of nitrogen fertilization treatments on conifer seedlings by foliar reflectance: a comparison of methods. *Tree Physiology* **20,** 1113–1120.

Munekaga Y, Hashimoto M, Miyaka C, Tomizawa KI, Endo T, Tasaka M, Shikanai T. 2004. Cyclic electron flow around photosystem I is essential for photosynthesis. *Nature* **429,** 579–582.

Nakaji T, Oguma H, Fujinuma Y. 2006. Seasonal changes in the relationship between photochemical reflectance index and photosynthetic light use efficiency of Japanese larch needles. *International Journal of Remote Sensing* **27,** 493–509.

Nichol CJ, Huemmrich KF, Black TA, Jarvis PG, Walthall CL, Grace J, Hall FG. 2000. Remote sensing of photosynthetic-light-use efficiency of boreal forest. *Agricultural and Forest Meteorology* **101,** 131–142.

Peguero-Pina JJ, Morales F, Flexas J, Gil-Pelegrin E, Moya I. 2008. Photochemistry, remotely sensed physiological reflectance index and de-epoxidation state of the xanthophyll cycle in Quercus coccifera under intense drought. *Oecologia* **156,** 1–11.

Peñuelas J, Filella I, Gamon JA. 1995. Assessment of photosynthetic radiation-use efficiency with spectral reflectance. *New Phytologist* **131,** 291–296.

Pfündel E, Bilger W. 1994. Regulation and possible function of the violaxanthin cycle. *Photosynthesis Research* **42,** 89–109.

R Development Core Team. 2010. *R: a language and environment for statistical computing* . Vienna, Austria: R Foundation for Statistical Computing.

Sarijeva G, Knapp M, Lichtenthater HK. 2007. Differences in photosynthetic activity, chlorophyll and carotenoid levels, and in chlorophyll fluorescence parameters in green sun and shade leaves of Ginkgo and Fagus. *Journal of Plant Physiology* **164,** 950–955.

Sims DA, Gamon JA. 2002. Relationships between leaf pigment content and spectral reflectance across a wide range of species, leaf structures and developmental stages. *Remote Sensing of Environment* **81,** 337–354.

Stylinski CD, Gamon JA, Oechel WC. 2002. Seasonal patterns of reflectance indices, carotenoid pigments and photosynthesis of evergreen chaparral species. *Oecologia* **131,** 366–374.

Yamamoto HY. 1979. Biochemistry of the violaxanthin cycle in higher plants. *Pure and Applied Chemistry* **51,** 639–648.